

New optical probe of GHz polarization dynamics in ferroelectric thin films

Charles Hubert and Jeremy Levy^{a)}

Department of Physics and Astronomy, University of Pittsburgh, Pittsburgh, Pennsylvania 15260

(Received 6 April 1999; accepted for publication 13 May 1999)

We describe a method for measuring the response of ferroelectric thin films to microwave-frequency electric fields. A mode-locked Ti:sapphire laser is used to generate a microwave drive signal that is phase locked to an optical probe pulse. The induced polarization change in the ferroelectric film is measured stroboscopically *via* the electro-optic effect. Images are acquired by scanning the laser beam across the sample in a confocal geometry. Time resolution is achieved by changing the delay between the electrical pump and the optical probe. Initial results show large local phase shifts in the ferroelectric response of closely separated (1 μm) regions of a $\text{Ba}_{0.5}\text{Sr}_{0.5}\text{TiO}_3$ thin film. This new experimental technique may help to understand the physical mechanisms of dielectric loss in these materials. © 1999 American Institute of Physics. [S0034-6748(99)00809-6]

I. INTRODUCTION

Ferroelectrics are promising materials for a number of applications. Their interesting properties are related to a structural phase transition which results in a spontaneous reversible electric polarization below a critical temperature T_c . Current and potential applications for ferroelectric materials include nonvolatile memory elements,¹ optical waveguides,² and electro-optic modulators.³ In the high-temperature (paraelectric) phase, the dielectric constant is large and highly nonlinear. The nonlinearity arises from a field-induced hardening of the soft transverse optical phonon mode,⁴ and can be exploited to make field-tunable capacitor elements.⁵⁻⁸ However, the dielectric loss in ferroelectric thin films is still too large for them to be useful in real devices. It is therefore important to understand the physical mechanisms of dielectric loss in ferroelectric thin films.

Optical techniques have been widely used in the study of ferroelectrics.⁴ In particular, stroboscopic methods were employed soon after the discovery of many of the most widely investigated materials such as BaTiO_3 . The first time-resolved work was performed at 60 Hz by Merz.⁹ The availability of pulsed lasers has allowed such stroboscopic methods to be extended to much higher frequencies. High-frequency electro-optic (EO) sampling methods have been widely exploited in other systems in recent years due to the increasing availability of ultrafast laser sources. Such sampling methods have been used in probe¹⁰ designs to monitor electronic currents at microwave frequencies. EO sampling of surface fields generated by photoexcited electron-hole pairs have also been used.¹¹ The sensitivity of EO probes is remarkable: they have even been used to detect the propagation of single flux quanta in superconducting circuits.¹² EO methods have a distinct advantage over purely electronic probes in that they can be used to *image* transient current densities in microwave circuits.¹³ Near-field mapping of the fields from microwave coplanar resonators has been demonstrated;¹⁴ also, near-field scanning optical microscopy

(NSOM) has been used with picosecond light sources to characterize microwave devices.¹⁵ For the investigation of ferroelectric thin films, it is the electro-optic response itself that is of interest, because it provides a direct measure of the ferroelectric polarization in the thin film.

II. EXPERIMENTAL METHOD

Here we describe a method for probing the polar response of ferroelectric thin films such as $\text{Ba}_x\text{Sr}_{1-x}\text{TiO}_3$. The method is based on confocal scanning optical microscopy (CSOM), a technique developed earlier for quasistatic imaging of ferroelectric polarization in thin films.¹⁶ With CSOM, both the sign and the magnitude of the linear electro-optic coefficient serve as a direct probe of the ferroelectric polarization.

Figure 1(a) shows a video micrograph of a typical ferroelectric thin film with interdigitated electrodes (light gray). The thin film (darker gray) serves as a dielectric between the two electrodes. In our experiments, a microwave voltage $V(t)$ is applied to the film. This voltage is derived from the pulse train of a mode-locked Ti:sapphire laser (frequency $f_1 = 76$ MHz) and is phase locked to a harmonic $f_n = nf_1$ of the fundamental repetition rate. The optical pulses are essentially delta functions in time, with a pulse width on the order of 100 fs. As shown in Fig. 1(b), the pulses from the Ti:sapphire laser are focused to a diffraction-limited spot on the sample. The change in polarization state of the reflected light can subsequently be related to the ferroelectric polarization at one particular phase of the microwave field.¹⁶ (We measure the birefringence rather than the reflectivity change as was described in Ref. 16 because it reduces the common-mode laser noise.) The phase between the microwave drive signal and the optical pulse is varied using an electrical delay line. Because the birefringence change due to $V(t)$ is small ($\sim 10^{-5}$), it is important to use noise-reduction techniques such as lock-in detection. Therefore, we amplitude modulate the microwave signal and lock-in detect at the modulation frequency ($f_{\text{mod}} = 100$ kHz). The lock-in signal therefore

^{a)}Electronic mail: jlevy@pitt.edu

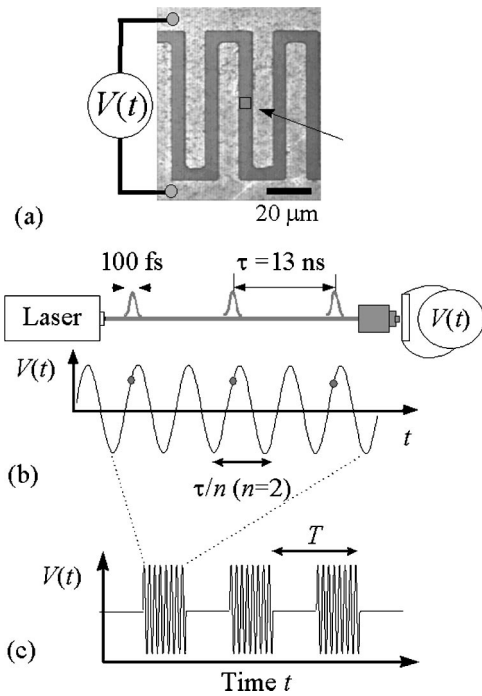


FIG. 1. (a) Video micrograph of a ferroelectric thin film with interdigitated electrodes. Light regions indicate electrodes, while dark regions indicate bare ferroelectric thin film. Boxed region indicates area over which images are acquired. (b) Schematic of time-resolved arrangement. (c) The driving voltage $V(t)$ is modulated to allow for phase sensitive detection with a lock-in amplifier.

measures the difference in ferroelectric polarization with and without the applied field.

Figure 2 shows a detailed schematic of how the experiments are performed. The output of the Ti:sapphire laser (Coherent Mira 900) is sent through an optical isolator and vertical polarizer (not shown) and split into two beams. The reflected beam is used to generate an electrical signal at the repetition rate of the laser ($f_1 = 76$ MHz) by detecting the pulses with a fast photodiode. The resulting signal is filtered and sent to a YIG-based tunable phase-locked oscillator (PLO) (Micro-Lambda MLSO-1132). This device can produce an output signal that is phase locked to a high harmonic n of the input frequency (output 2–4 GHz). Using a different PLO it is possible to generate phase-locked outputs up to 40 GHz. The PLO output is sent through an analog electrical delay line (Gigabaudics PADL) which can be varied from 0 to 10 230 ps in steps of 10 ps. Both the PLO frequency and the electrical delay line are computer controlled. Finally, the

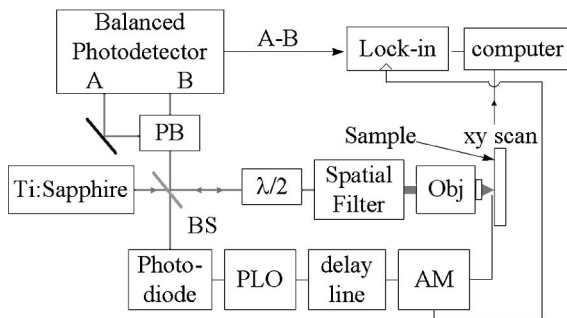


FIG. 2. Block diagram of experimental setup.

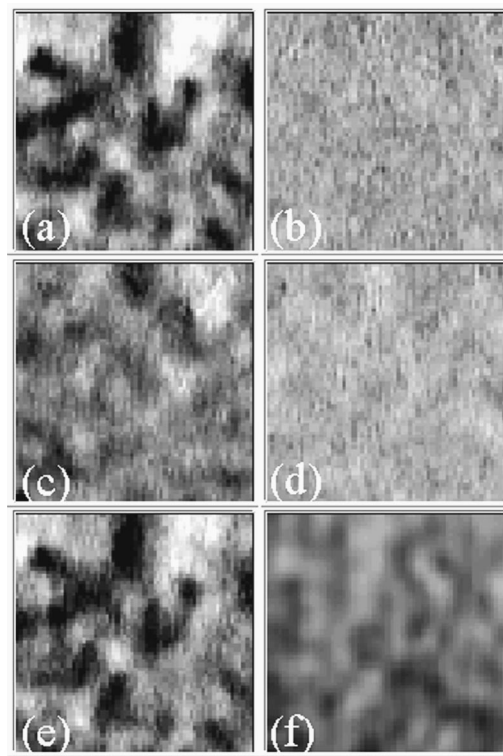


FIG. 3. Time-resolved images of $\text{Ba}_{0.5}\text{Sr}_{0.5}\text{TiO}_3$ thin film at different delays between the electrical “pump” and optical probe. Images are $5 \mu\text{m} \times 5 \mu\text{m}$ in size. (a) $t = 0$ ps. (b) $t = 120$ ps. (c) $t = 240$ ps. (d) $t = 360$ ps. (e) $t = 480$ ps. (f) DC reflectivity image of the film at $t = 0$ ps. Variations in intensity are small ($<10\%$).

output is square-wave modulated at f_{mod} using a 50Ω GaAs switch and sent to the electrode pattern on the sample.

The transmitted output from the same beamsplitter is directed toward the sample. A half-wave plate rotates the polarization by 45° with respect to the microwave electric field. The beam is then sent through a spatial filter and beam expander and focused to a diffraction-limited spot (~ 500 nm) using a high numerical aperture objective ($\text{NA} = 0.85$). The reflected light passes through the same spatial filter in a confocal arrangement, further enhancing the spatial resolution. A polarizing beamsplitter, oriented at 45° with respect to the polarization axis of the incident light, separates the light into two orthogonally polarized beams which are directed to a balanced pair of Si photodiodes (labeled A and B). The reference signal A is monitored while the difference signal A-B is sent to a lock-in amplifier. The reference frequency for the lock-in amplifier is used to modulate the amplitude of the microwave signal, which in turn modulates the A-B signal. The computer controls the locking multiple n , the electrical delay, the x , y , and z position of the sample (adjusted for maximum reflected light), and the acquisition of signals from the lock-in amplifier and other sources. Images are acquired by raster scanning in the x and y directions.

III. EXPERIMENTAL RESULTS

Images acquired at a particular phase of the driving microwave field give qualitative insight into the dynamical response of the ferroelectric thin film on picosecond time

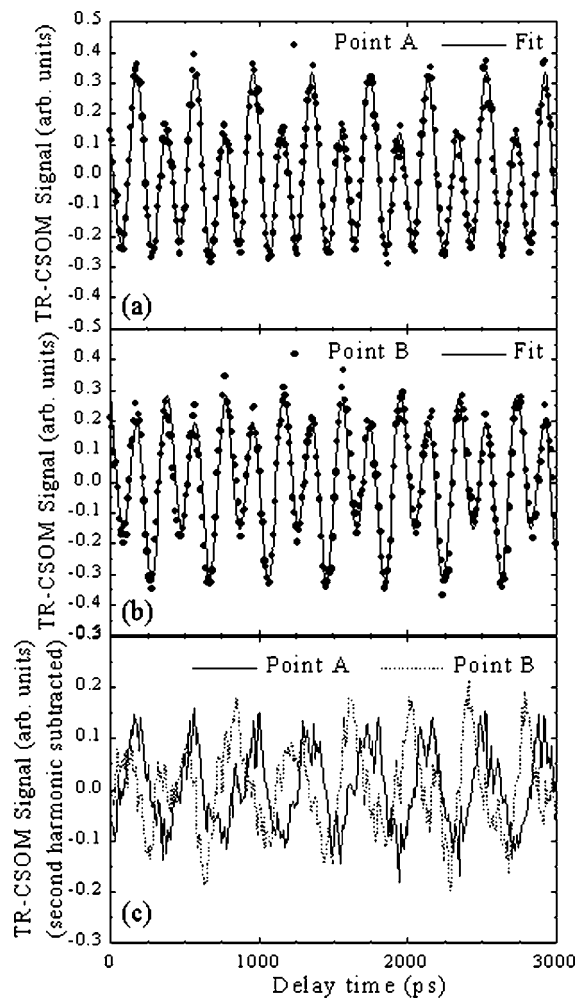


FIG. 4. (a) Time-resolved signal obtained at a single location A. Solid line shows a fit to a sinusoidal function at the fundamental and the second harmonic. (b) Time-resolved signal obtained at a nearby ($1 \mu\text{m}$ separation) location B. (c) Comparison of fundamental response of locations A and B. The response at the second harmonic has been subtracted from both curves, and a noticeable phase shift is observed.

scales. The film studied here is a 500 nm thick $\text{Ba}_{0.5}\text{Sr}_{0.5}\text{TiO}_3$ film deposited epitaxially onto an MgO substrate using off-axis sputtering. Figure 3 shows a sequence of five images taken over a $(5 \mu\text{m})^2$ area at various electrical delays. In this series of images, the microwave field (amplitude 10 $\text{kV}_{\text{rms}}/\text{cm}$) is oriented at an angle of 45° with respect to horizontal, with a frequency $f_{27}=2.038$ GHz. At $t=0$ ps [Fig. 3(a)], the response is large, because at this phase in the cycle the applied field is close to a maximum. The appearance of positive (bright) and negative (dark) regions is due to the fact that the ferroelectric domains can have a component that is either parallel or antiparallel to the electric field. That is, the electric field causes the magnitude of the polarization to increase in one case, and decrease in the other. At $t=120$ ps [Fig. 3(b)], the response has almost disappeared because the field is near a zero crossing in the driving field. At $t=240$ ps [Fig. 3(c)], the drive has changed by approximately half a cycle compared to $t=0$. Note that there is not a simple reversal in all of the regions. Rather, there is in addition a strong second harmonic response. This contribution to the response is due to regions which are either

TABLE I. Coefficients for fits to data shown in Fig. 4. The fit is to the functional form: $S(t)=A_1 \cos(2\pi f_n t + \phi_1) + A_2 \cos(4\pi f_n t + \phi_2)$.

	A_1	A_2	ϕ_1	ϕ_2
Point A	0.099	0.237	1.00	1.40
Point B	0.093	0.236	2.90	1.44

paraelectric or have their ferroelectric polarization perpendicular to the applied field (e.g., c -axis oriented). In such cases one would expect a quadratic dependence of the measured signal on the applied field. At $t=360$ ps [Fig. 3(d)], we see very similar behavior to Fig. 3(b), since we are probing the second zero crossing. At $t=480$ ps [Fig. 3(e)], the image is nearly identical to that shown in Fig. 3(a). This result is to be expected because of the periodic nature of the excitation. Figure 3(f) shows an image of the average sample reflectivity. Variations are small (on the order of 10%), and are used to ensure that the time-resolved images, when compared, are in good registry.

More quantitative information may be obtained by collecting data at a fixed position on the sample while varying the electrical delay. Figures 4(a) and 4(b) show two such curves taken at points separated by $1 \mu\text{m}$. The response is periodic with the expected period. Although there are clearly higher harmonics, the data can be fitted well to an amplitude and phase of the fundamental and second harmonic, shown in Figs. 4(a) and 4(b) as a solid line. Table I lists the values of the fit for the two curves shown. The second-harmonic amplitude and phase are comparable for the two curves, as are the amplitudes of the fundamental. The phase of the fundamental response is significantly different, and can be clearly seen by comparing points A and B with the second harmonic response subtracted [Fig. 4(c)].

IV. DISCUSSION

An understanding of the physical origin of the local phase shifts observed may help in reducing dielectric loss in these materials. For example, local variations in stress are known to manifest themselves as random local electric fields which can lead to glassy “relaxor” behavior.¹⁷ More detailed studies as a function of frequency, temperature, and driving amplitude may help to clarify the role of ferroelectric domains in producing dielectric loss. The time-resolved technique described here can also be combined with higher spatial resolution probes such as apertureless near-field scanning optical microscopy¹⁸ to provide further insights into the mechanisms of dielectric loss in these materials.

ACKNOWLEDGMENTS

This work was supported by ONR (N00173-98-1-G001) and the National Science Foundation (DMR-9701725). The authors also thank Ed Cukauskas and Steve Kirchoefer (Naval Research Laboratory, Washington, DC 20375) for providing the patterned ferroelectric thin films.

¹J. F. Scott, *Ferroelectrics Rev.* **1**, 1 (1998).

²B. H. Hoerman, G. M. Ford, L. D. Kaufmann, and Y. B. W. Wessels, *Appl. Phys. Lett.* **73**, 2248 (1998).

- ³D. M. Gill, C. W. Conrad, G. Ford, B. W. Wessels, and S. T. Ho, *Appl. Phys. Lett.* **71**, 1783 (1997).
- ⁴M. E. Lines and A. M. Glass, *Principles and Applications of Ferroelectrics and Related Materials* (Clarendon, Oxford, 1977).
- ⁵V. K. Varadan, D. K. Ghodgaonkar, V. V. Varadan, J. F. Kelly, and P. Glikerdas, *Microwave J.* **35**, 116 (1992).
- ⁶R. W. Babbitt, T. E. Koscica, and W. C. Drach, *Microwave J.* **35**, 63 (1992).
- ⁷K. R. Carroll, J. M. Pond, D. B. Chrisey, J. S. Horwitz, R. E. Leuchtner, and K. S. Grabowski, *Appl. Phys. Lett.* **62**, 1845 (1993).
- ⁸J. S. Horwitz, D. B. Chrisey, J. M. Pond, R. C. Y. Auyeung, C. M. Cotell, K. S. Grabowski, P. C. Dorsey, and M. S. Kluskens, *Integr. Ferroelectr.* **8**, 53 (1995).
- ⁹W. J. Merz, *Phys. Rev.* **95**, 690 (1954).
- ¹⁰M. Shinagawa and T. Nagatsuma, *Instrumentation/Measurement Technology Conference*, Waltham, MA, 1995 (IEEE, New York, 1995), pp. 324–328.
- ¹¹G. L. Eesley, *J. Appl. Phys.* **82**, 6078 (1997).
- ¹²C. C. Wang, M. Currie, D. Jacobs-Perkins, M. J. Feldman, R. Sobolewski, and T. Y. Hsiang, *Appl. Phys. Lett.* **66**, 3325 (1995).
- ¹³P. Campbell, M. Li, Z. G. Lu, J. A. Riordan, K. R. Stewart, G. A. Wagoner, J. Wu, and X. C. Chang, *Commercial Applications of Ultrafast Lasers*, San Jose, CA, 1998, pp. 114–125.
- ¹⁴T. Pfeifer, T. Löffler, H. G. Roskos, H. Kurz, M. Singer, and E. M. Biebl, *IEEE Trans. Antennas Propag.* **46**, 284 (1998).
- ¹⁵C. Bohm, J. Bangert, W. Mertin, and E. Kubalek, *J. Phys. D* **27**, 2237 (1994).
- ¹⁶C. Hubert, J. Levy, A. C. Carter, W. Chang, S. W. Kiechoefer, J. S. Horwitz, and D. B. Chrisey, *Appl. Phys. Lett.* **71**, 3353 (1997).
- ¹⁷V. Westphal, W. Kleemann, and M. D. Glinchuk, *Phys. Rev. Lett.* **68**, 847 (1992).
- ¹⁸C. Hubert and J. Levy, *Appl. Phys. Lett.* **73**, 3229 (1998).